***Case 1:*** $X_F > X_G$

$$M_3 = \frac{-X_F(Y_F - Y_A) \pm r_{cx}[X_F^2 + (Y_F - Y_A)^2 - r_{cx}^2]^{1/2}}{r_{cx}^2 - X_F^2} \tag{14}$$

The coordinates of points $A$ and $F$ are

$$X_A = 0 \tag{15}$$

$$Y_A = (r_p^2 - r_{cx}^2)^{1/2} \tag{16}$$

$$X_F = (r_p^2 - r_{cv}^2)^{1/2} \sin(a + b) - r_{ccv} \cos(e - a - b) \tag{17}$$

$$Y_F = (r_p^2 - r_{ccv}^2)^{1/2} \cos(a + b) + r_{ccv} \sin(a + b - e) \tag{18}$$

The angle $(a + b)$ corresponds to the section of the circle of radius $R_p$ taken up by one-half concave and one-half convex fins Analytically, $(a + b)$ is

$$a + b = \sin^{-1}(r_{cx}/r_p) + \sin^{-1}(r_{ccv}/r_p)$$

Note that Eq (14) provides two values of $M_3$ The smaller one is the correct one to use

***Case 2:*** $X_F < X_G$

$$M_3 = (Y_G - Y_F)/(X_G - X_F) \tag{19}$$

$M_4$ is calculated from the equation

$$-(X_F - X_B)(Y_F - Y_B) \pm M_4 = \frac{r_{cx}[(Y_F - Y_B)^2 + (X_F - X_B)^2 - r_{cx}^2]^{1/2}}{r_x^2 - (X_F - X_B)^2} \tag{20}$$

Note that Eq (20) provides two values of $M_4$ The greater value is the correct one to use

### Fin Effectiveness

The following equation is used as an approximate measure of the effectiveness of a finned surface:

$E_f$ = effective (approximate) fin efficiency =

$$\frac{A_{ccv}F_{ccv} + A_{cx}F_{cx}}{A_p} \tag{21}$$

where $A_p$ is the outer surface of nonfinned cylinder, ft² After some manipulations, the following final equation is obtained:

$$E_f = \frac{r_{cx}F_{cx} + r_{ccv}F_{ccv}}{R_p(a + b)/90} \tag{22}$$

where $a = \sin^{-1}(r_x/r_p)$ and $b = \sin^{-1}(r_v/r_p)$

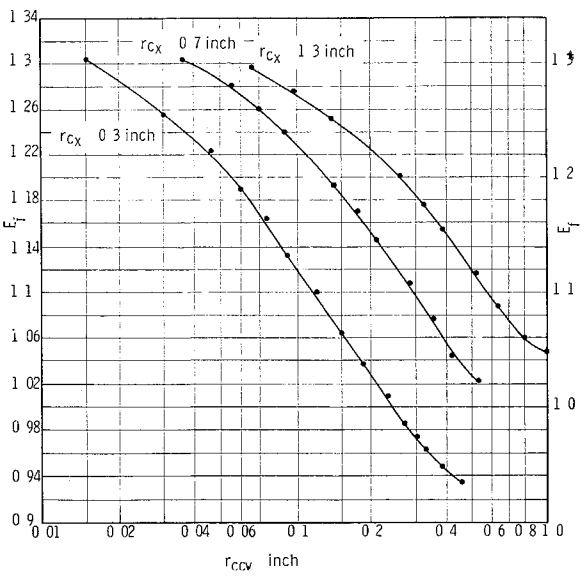


**Fig 2 Fin efficiency as function of convex and concave radii ($R_p$ = 5 in )**

### Calculations

The equations shown were programmed for the IBM 704 computer, and the fin efficiency for various values of $R_p$, $r_x$, and $r$ was calculated The results of the computations are shown in Fig 2 It is worth noting that although Fig 2 is based on a radius $R_p$ of 5 in , it is applicable to any radius $R_p$ in view of the following fact: if $[(r_x)_1/(R_p)_1] = [(r_x)_2/(R_p)_2]$ (where the subscripts 1 and 2 refer to different finned surfaces) and $[(r_x)_1/(r_c)_1] = [(r_{cx})_2/(r_c)_2]$, then $(E_f)_1 = (E_f)_2$

### Conclusions

An increase in the ratio of convex to concave fin radii always results in an improved fin efficiency

If two finned surfaces, denoted by the subscripts 1 and 2, are such that

$$[(r_x)_1/(r\ )_1] = [(r_x)_2/(r\ )_2]$$

and

$$[(r_x)_1/(R_p)_1] = [(r_x)_2/(R_p)_2]$$

then $(E_f)_1 = (E_f)_2$

### Reference

[1] Jakob, M , *Heat Transfer* (John Wiley and Sons, Inc , New York, 1957), Vol II, pp 6–9

# Integral Equations for Viscous Hypersonic Nozzle Flow

M Sichel*
*University of Michigan, Ann Arbor, Mich*

Schlichting[1] has shown that in incompressible diffusers the integral equations for the combined core and boundary-layer flows have the same form as the usual boundary-layer integral equations In the present note it is shown that this result remains valid in conical hypersonic nozzles in which the thick hypersonic boundary layers and the core flow interact

Following Schlichting[1] the conservation equations will be simultaneously formulated for both the core and boundary-layer flows Since the boundary layer thickness is of the same order as the nozzle radius, the effect of transverse curvature, which has been discussed by Durand and Potter[2] and by Michel,[3] must be taken into account The coordinate system used is shown in Fig 1 and is the same as that in Refs 2 and 3 In the case of turbulent flow all parameters are temporal averages

The flow is divided into a useful inviscid core and a boundary layer of thickness $\delta$ It is assumed that the core flow behaves as a spherical source even when the boundary layer

Received September 30, 1963 The work reported here was sponsored by the Office of Naval Research under Contract Nonr-1224(31) NR 061-108

* Assistant Professor, Department of Aeronautical and Astronautical Engineering Member AIAA

is thick Indications are that this assumption is not unreasonable [4] Then the total mass flow $\dot{m}$ through the boundary layer and the core is given by

$$\dot{m} = \int_0^{\delta} 2\pi\, r\rho u dy + \int_0^{\theta_{uc}} 2\pi R^2 \rho_e V_e \sin\theta\, d\theta \qquad (1)$$

As in Refs 2 and 3, a displacement thickness $\delta_1$ is defined by

$$\int_0^{\delta_1} 2\pi r\rho\, u_e dy = \int_0^{\delta} 2\pi r(\rho_e u_e - \rho u) dy \qquad (2)$$

If, as is usually the case, $\theta_w \ll 1$, it can be shown that[5]

$$\dot{m} = \pi\rho\, V_e(R - \delta_1)^2[1 + O(\theta_w^2)] \qquad (3)$$

Consequently, the mass flow is approximately

$$\dot{m} = \pi\rho\, u_e(R - \delta_1)^2 = \pi\rho_e u_e R(R - 2\bar{\delta_1}) \qquad (4)$$

where

$$\bar{\delta_1} = \delta_1 - \delta_1^2/2R$$

Equation (4) is thus the continuity equation for the nozzle

In formulating the momentum and energy equations it will be assumed at the outset that $\theta_w \ll 1$ so that the nozzle velocity distribution is approximately as shown in Fig 2 With $\theta_w \ll 1$, Eq (2) defining the displacement thickness can be written as

$$\delta_1 - \frac{\delta_1^2}{2R} = \bar{\delta_1} = \int_0^R \frac{r}{R}\left(1 - \frac{\rho u}{\rho_e u_e}\right) dr \qquad (5)$$

and as long as there is a uniform inviscid core extending the upper limit of the integral in Eq (5) from $\delta$ to $R$ has no effect on the results A momentum thickness is defined as in Refs 2 and 3 by the relation

$$\int_0^{\delta_2} 2\pi r(\rho\, u_e^2) dy = \int_0^{\delta} 2\pi r\rho(u_e u - u^2) dy \qquad (6)$$

which reduces to

$$\delta_2 - \frac{\delta_2^2}{2R} = \bar{\delta_2} = \int_0^R \frac{\rho u}{\rho_e u_e}\left(1 - \frac{u}{u}\right)\frac{r}{R} dr \qquad (7)$$

Application of conservation of momentum to a control volume of length $dx$ (see Fig 2) yields the equation

$$\frac{d}{dx}\left[\int_0^R 2\pi\rho u^2 r dr\right] = -\pi R^2 dp - \tau_w 2\pi R dx \qquad (8)$$

Combination of the continuity equation with Eq (8) yields the following equation for the conservation of momentum in the combined core and nozzle flows

$$\frac{d\bar{\delta_2}}{dx} + \bar{\delta_2}\left[\frac{\bar{H} + 2}{u_e}\frac{du_e}{dx} + \frac{1}{\rho}\frac{d\rho_e}{dx} + \frac{1}{R}\frac{dR}{dx}\right] = \frac{C_f}{2} + \frac{R}{2\rho\, u_e^2}\left(\frac{dp}{dx} + \rho\, u_e \frac{du_e}{dx}\right) \qquad (9)$$

where $\bar{H} = \bar{\delta_1}/\bar{\delta_2}$

A key assumption used in deriving Eq (9) is that the pressure across the boundary layer is constant and equal to that in the core, even in the case where $\delta/R \sim O(1)$ In the laminar case

$$(\partial p/\partial y)/(\partial p/\partial x) \sim \delta/L$$

where $L$ is some dimension characterizing the rate of variation of $p_e$ with $x$, such as the nozzle length Even with $\delta/R \sim O(1)$, the constant pressure assumption should remain valid provided $R/L \ll 1$ The pressure change across a turbulent boundary layer is if the order[6]

$$\Delta p/p_e \sim \gamma M_e^2(\overline{v^2}/\bar{\rho}\, u_e^2)$$

where $\overline{v^2}/u_e^2$ is the turbulence level For large $M_e$ the turbulence level must thus be extremly small if the constant pressure assumption is to hold

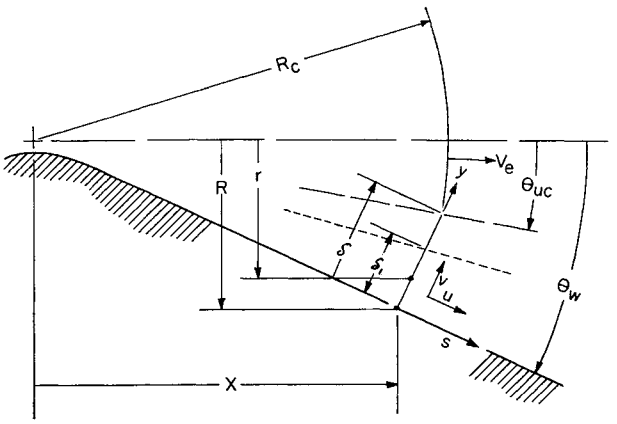


**Fig 1 Conical nozzle boundary-layer coordinate system**

Since the core flow is inviscid and one dimensional to the present order of approximation

$$dp/dx = -\rho_e u_e(du_e/dx)$$

so that Eq (9) becomes

$$\frac{d\bar{\delta_2}}{dx} + \bar{\delta_2}\left[\frac{\bar{H} + 2}{u}\frac{du_e}{dx} + \frac{d}{dx}(\ln\rho\, R)\right] = \frac{C_f}{2} \qquad (10)$$

Thus, with an inviscid core the integral momentum equation for the entire nozzle reduces to the same form as the boundary-layer momentum integral equation, as was also found by Schlichting[1] for incompressible diffuser flow If $h_o$ is the total enthalpy, application of the conservation of energy to the control volume in Fig 2 yields

$$\frac{d}{dx}\left[\int_0^R 2\pi\, r\rho u h_o dr\right] = 2\pi R q_w \qquad (11)$$

where $q_w$ is the heat flux per unit area from the wall to the fluid Definition of an energy thickness $\delta_3$ by

$$\int_0^{\delta_3} 2\pi\, r\rho_e u_e h\, dy = \int_0^{\Delta} 2\pi\, r\rho u(h_o - h_{oe}) \qquad (12)$$

as is done in Shapiro[7] leads to the relation

$$\delta_3 - \frac{\delta_3^2}{2R} = \bar{\delta_3} = \int_0^R \frac{\rho u}{\rho_e u_e}\frac{r}{R}\left(\frac{h_o}{h_{oe}} - 1\right) dr \qquad (13)$$

where $\Delta$ is the thermal boundary-layer thickness Combining (13) and (11) leads to

$$\frac{d\bar{\delta_3}}{dx} + \bar{\delta_3}\frac{d}{dx}(\ln\rho_e u\, R) = \frac{q_w}{\rho_e u_e h_o} \qquad (14)$$

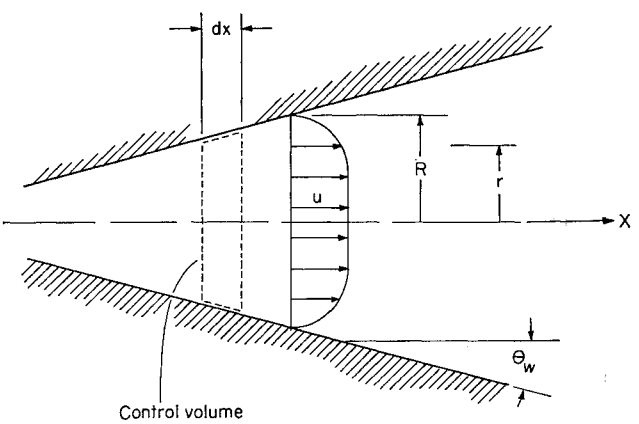


**Fig 2 Approximate nozzle velocity distribution for the case $\theta_w \ll 1$**

Determination of the nozzle flow now requires simultaneous solution of Eqs (4, 10, and 14) for $\bar{\delta}_1$, $\bar{\delta}_2$, and $u$ These equations are closely related to the ordinary boundary-layer integral equations; however, while $u$ (the external velocity) is usually known, the nozzle problem is complicated by the fact that the variation of $u_e$ is itself dependent upon the solution of Eqs (10) and (14) since $u_e$ must satisfy Eq (4) for the conservation of mass

In the turbulent case it will generally be necessary to introduce empirical assumptions regarding the velocity distribution through the boundary layer and the skin friction coefficient The energy equation may be replaced by the assumption that Crocco's relation between velocity and enthalpy is valid

### References


[1] Schlichting, H , "Berechnung der Strömung in rotationsymmetrischen Diffusoren mit Hilfe der Grenzschicht theorie," Z Flugwissenschaften 9, n 4/5 (1961)

[2] Durand, J A and Potter, J L , "Calculation of thicknesses of laminar boundary layers in axisymmetric nozzles with low density, hypervelocity flows," Arnold Eng Dev Center, AEDC-TN-61-146 (December 1961)

[3] Michel, R , "Developpement de la couche limite dans une tuyere hypersonique," *AGARD Specialists Meeting High Temperature Aspects of Hypersonic Flow, Rhode Saint Genese, Belgium* (Pergamon Press Ltd , London, 1963)

[4] Burke, A F and Bird, K D , "The use of conical and contoured expansion nozzles in hypervelocity facilities," *Proceedings of Second Symposium on Hypervelocity Techniques; Advances in Hypervelocity Techniques* (Plenum Press, New York, 1962), pp 373–424

[5] Sichel, M , "The effect of the boundary layer upon the flow in a conical hypersonic wind tunnel nozzle," Univ Mich , Office of Res Administration Rept 02953-2-F (July 1963)

[6] Schubauer, G B and Tchen, C M , "Turbulent flow," *High Speed Aerodynamics and Jet Propulsion; Turbulent Flows and Heat Transfer*, edited by C C Lin (Princeton University Press, Princeton, N J , 1959), Vol V

[7] Shapiro, A H , *The Dynamics and Thermodynamics of Compressible Fluid Flow* (Ronald Press, New York, 1954), Vol II, p 1092


# A Simple Geometric Method for Analyzing Polarization States in Photoelasticity


ROBERT MARK*

*Princeton University, Princeton, N J*


IN the photoelastic model analysis of thin shells such as those employed for typical rocket structures, it is frequently necessary to account for the effect of rotating principal stress axes through the shell wall in regions where the principal shell membrane forces are not acting along the same axes as the principal bending moments The procedure described in this note, which has had important application in the field of crystal-optics[1] and electrical engineering,[2] can be utilized to give particular solutions for the shell problem, as well as providing clear understanding of other polarization phenomena observed in general photoelasticity

Linearly polarized light passing through the strained birefringent element shown in Fig 1 is split into components along the principal stress axes $x$, and $y$ The field $E_y$ is seen to lead $E_x$ by the phase difference $\delta\lambda$, since the propagation velocity through the strained element along the $y$-principal stress axis is greater than that of the component along the

Received October 7, 1963

* Lecturer, Department of Civil Engineering

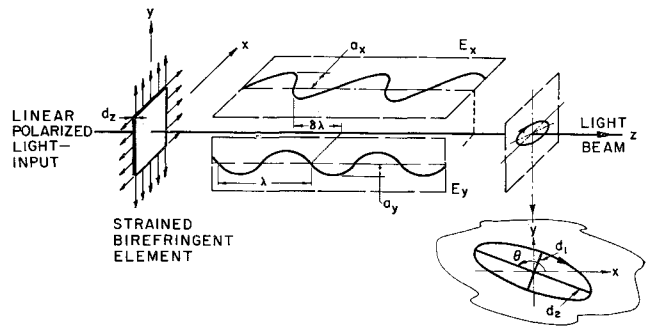


**Fig 1 Polarization output from a strained birefringent element**

$x$ axis In this case, the $y$ axis is referred to as the fast axis of the element

The ratio of the amplitudes of the field components $a_x, a_y$ depends on the orientation of the element with respect to the polarizing axis; the phase difference is a function of the wavelength of the light employed, material properties and thickness of the element $dz$, and the principal stress differences along the light path These relationships are derived in standard photoelasticity texts

Resolution of the components along the light beam $z$ axis at a particular instant forms a helix which when viewed from the outer end of the beam is seen as an ellipse The "elliptical" polarization thus formed is defined as "right-handed" if the helix has the form of a right-handed screw thread, and left-handed if it is of the opposite hand

The state of polarization may be completely described by giving its handedness along with the azimuth of the major

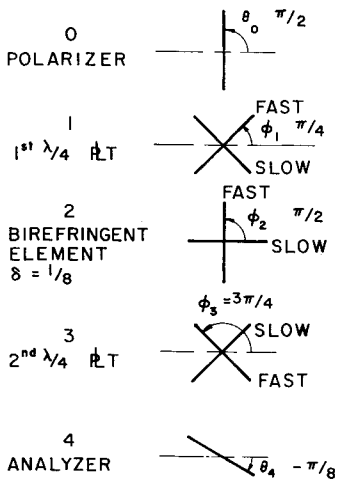


**Fig 2a Arrangement of circular polariscope for tardy compensation**

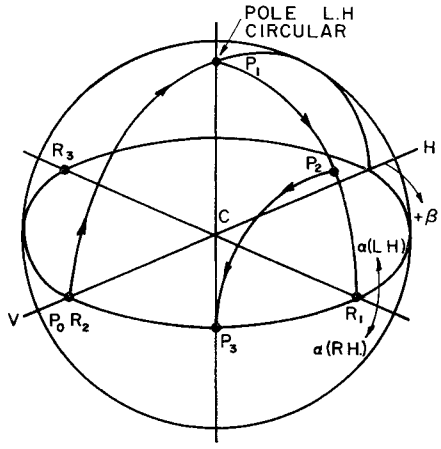


**Fig 2b Poincaré sphere solution of Fig 2a**